Preprint version of:
I. Diez-de-los-Rios, A. Suarez, E. Sanchez-Laulhe, I. Armengol and A. Ollero, "Winged Aerial Robot: Modular Design Approach," 2021 IEEE International Symposium on Safety, Security, and Rescue Robotics (SSRR), 2021, pp. 190-195

Winged Aerial Robot: Modular Design Approach

Ivan Diez-de-los-Rios, Alejandro Suarez, Ernesto Sanchez-Laulhe, Inmaculada Armengol, Anibal Ollero[1]

***Abstract*—This paper presents the design, modelling, control, and experimental validation of a novel flapping wing aerial robot built with servo actuators that could be applied in search, rescue, and assistance to injured people. The proposed concept design is intended to facilitate the construction of this kind of aerial robots following a modular and reconfigurable approach, consisting of a series of Servo-Flapping Engine (SFE) modules attached to the carbon fibre tube used as fuselage, and a tail servo, covering the structure with a light nylon cloth. The SFE modules are built with a pair of servos that rotate the wing rods with desired amplitude, frequency, and relative phase. Combining two SFE modules, it is possible to generate different flapping patterns and control the orientation of the aerodynamic surfaces. The paper covers the parametrization of the design, the hardware/software implementation, as well as the modelling and control. The proposed design is validated through gliding and flapping tests in an outdoor environment.**

***Index Terms*—Aerial Robotics, Flapping-Wing Aerial Robot**

I. Introduction

FLAPPING-WING robots represent a new generation of biologically inspired aerial platforms [1], [2], [3], [4], [5] intended to overcome the current limitations of multirotors in terms of energy efficiency [6] and safety [7]. It is expected that in a near future aerial robots will be capable of interacting closely and safely with the humans in urban environments [8], flying along streets and roads to conduct search and rescue operations and perform some kind of manipulation task [9], [10] to provide assistance to injured people, like the delivery of first-aid kits, oxygen masks and pulse oxygen sensors, or taking samples from the environment. The idea of using such kind of robots in urban environments results of interest for a wide variety of applications where multirotors may not be suitable due to their limited flight time and the risk of their propellers for humans in case of failures or malfunctions. The ability of winged aerial robots to glide with no energy consumption reduces the kinetic energy and, consequently, the potential damage from an impact. The relatively low flight speed compared to fixed-wing unmanned aerial vehicles (UAVs) also facilitates the navigation between buildings and landing on small areas.

In the development of this kind of robots it is possible to identify two approaches depending on the way the flapping-wing mechanism is implemented. On the one hand, some works [1], [3], [4] employ a single motor in continuous rotation with a reduction gearbox and a transmission mechanism that converts the rotational motion into the flapping motion. In this case, both wings rotate simultaneously and synchronously, requiring the integration of additional actuators to achieve roll/yaw control. On the other hand, reference [2] proposes the use two RC digital servos to achieve independent wing control, avoiding the need of building an external gearbox. However, this implementation is affected by the limitations of conventional RC servos that only provide position control with no feedback.

Figure 1. Winged aerial robot built with two servo flapping engines.

The Bat-Bot robot presented in [11] follows a bio-inspired approach, considering the kinematics and biomechanical parameters of bats for the design of the wing mechanism. The winged aerial manipulation robot developed in our previous work [10] proposes a double functionality for the dual arm, manipulating and gliding, removing the distinction between the aerial platform and manipulator to reduce the total weight.

The main contribution of this paper is the development of a flapping-wing aerial robot (Winged AR) built with smart servo actuators, following a modular design approach that facilitates the manufacturing of platforms according to the power requirements or the weight constraints, distributes the load of the actuators, and increases fault tolerance. The main bio-mechanical parameters of the winged aerial robot are firstly identified based on studies on different bird species. The concept of servo flapping engine (SFE) is then introduced as the core of the modular design and related to the mentioned parameters. The paper shows how combining two SFEs it is possible to generate different flapping patterns with desired amplitude, dihedral angle, frequency and phase, allowing to change the aerodynamic surfaces to achieve better manoeuvrability in the lateral gliding control (roll/yaw). A prototype of winged aerial robot built with two SFEs and an actuated tail for pitch control is developed, showing gliding and flapping experiments in outdoors.

[1]GRVC Robotics Labs, University of Seville, Spain. https://grvc.us.es/

The rest of the paper is organised as follows. Section II presents the design principles, describing in Section III the development of the prototype, which comprises the servo flapping engine, the wing structure, and the electronics. Section IV covers the aerodynamic modelling and control of the robot. Experimental results are presented in Section V, summarising the conclusions in Section VI.

II. Design Principles

A. Characterisation of Winged Aerial Robot

In the design of a flapping wing aerial robot, it is useful to identify and analyse the bio-mechanical parameters of interest of different birds that can be assimilated to the aerial platform in terms of size and weight in order to estimate the sizing of the flapping wing mechanism. Reference [12] compares the weight, wingspan, flight speed and power of different bird species whose weight is in the range of the aerial robot presented in this paper.

Formally, we will characterise the design of the flapping wing aerial platform by the following tuple of parameters:

$$DP_{platform} =< m,\ WS,\ f,\ v,\ P > \tag{1}$$

where m is the mass, WS is the wingspan, f is the flapping frequency, v is the nominal flight speed, and P is the power developed by the flapping engine.

Although the flight apparatus of birds is too complex to be properly replicated, it is possible to establish an analogy between the power generated by the shoulder muscles of the birds and the power delivered by a rotational servo actuator characterised by the following tuple of design parameters:

$$DP_{actuator} = < m_a,\ \tau_a^{max},\ \omega_a^{max},\ P_a > \tag{2}$$

where m_a is the actuator weight, τ_a^{max} and ω_a^{max} are the maximum dynamic torque and angular speed of the actuator, respectively, and P_a is the power of the actuator. Note that in most servo actuators commercially available, the manufacturer only provides the stall torque, that is, the maximum torque that can be supported in static conditions, taking advantage of the friction of the gearbox. However, in practice, the dynamic torque is usually 2 – 3 times lower than this value. The mechanical power of the actuator, P_a, is a representative parameter since it relates the torque delivered by the actuator with the angular speed, that is, with the flapping frequency f:

$$P_a = A \cdot f \cdot \tau_a \tag{3}$$

where A is the flapping wing amplitude (in rad). Taking into account that the angular speed of the servo is limited, it is easy to derive the following constraint in the amplitude:

$$A \leq \omega_a^{max}/f \tag{4}$$

Equations (3) and (4) are important because they determine the size of the wing needed to generate the required thrust (see Section IV), in such a way that if the angular speed of the servo is low, the wingspan should be high to compensate, and vice versa. The parametrisation of the aerial platform and the actuators given by Equations (1) and (2) allows the formulation of a modular design approach for the development of winged aerial robots. The idea is that the power of the aerial robot can be scaled with the number of actuators N as needed, knowing that the weight of the platform will increase almost proportionally ($m \propto N \cdot m_a$, $P \propto N \cdot P_a$). The main benefits of the modular approach proposed in this work are highlighted in the next subsection.

B. Modular Design Approach

Unlike the prototype presented in [3] that employs a single brushless motor to generate the thrust, and unlike [2] where a single servo pair is considered for flapping the wings, the winged aerial robot described in next section and whose features are compared in Table I is built with smart servo actuators following a modular approach motivated in the following terms:

1) Manoeuvrability: the independent position control of the servos allows the generation of different gliding and flapping patterns as well as the orientation of the aerodynamic surfaces to produce desired moments (see Figure 2), avoiding the need to include additional actuators to implement the roll/yaw control. The relatively low speed of the prototype (see Table I) also facilitates the accurate landing and perching compared to the one performed in [3].

2) Load distribution: the use of several actuators to move the wings reduces the stress supported by the tooth of the gears, particularly in the last stage of the gearbox, which contributes to extend the lifespan of the platform.

3) Energy efficiency: in relation to the previous point, and according to Table I, the motor employed to rotate both wings should compensate the friction and inertia of the external gearbox, whereas the power loss in a servo actuator is typically lower due to the integrated construction and the lubrication of the gears. In terms of power, the consumption in reference [3] is significantly higher than the Winged AR.

4) Simple manufacturing: the use of smart servo actuators that integrate the gearbox and control electronics in a compact device reduces the time and simplifies significantly the manufacturing of a this kind of platforms.

5) Fault tolerance: the redundancy in actuators is useful to improve reliability, in such a way that the platform can be controlled to glide and land safely if case of damage or fault, exploiting for this purpose the information provided by the smart servos. The torque control of the smart servos can be disabled to allow the free rotation of the shaft, driven by the other actuators of the same wing.

Table I
Comparison of three flapping-wing prototypes

Feature	Robird [3]	Robo Raven [2]	Winged AR
Num. actuators[1]	1	2	4
Weight [kg]	0.73	0.29	0.5
Power [W]	112	2 × 9.4	4 × 5
Flight speed [m/s]	16	6.7	5
Wingspan [m]	1.12	1.16	1.5

[1] Tail actuators not included.

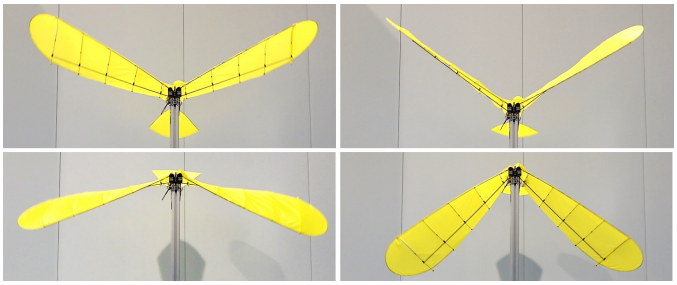

Figure 2. Flapping patterns generated changing the rod angles of the servo flapping engine pair.

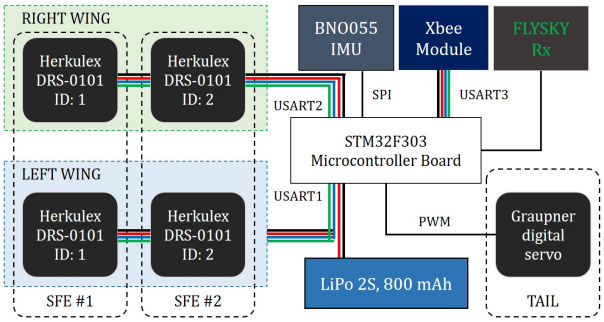

Figure 3. Hardware architecture of the winged aerial robot.

III. Structure and Design

A. Servo Flapping Engine (SFE)

The main component of the winged aerial robots presented in this paper is the servo flapping engine (SFE), an actuation module consisting of two Herkulex DRS-0201 smart servos (60 grams weight, 24 kgf·cm stall torque at 7.4 V) supported by a carbon fibre frame that can be attached to the fuselage tube through a Ruland aluminium shaft collar. Each of the servos rotate a thin carbon fibre rod where the nylon cloth of the wing is fixed. A picture of the mechanism is illustrated in Figure 1. The use of servo actuators for this purpose is motivated for three reasons: 1) these servos integrate the motor, gearbox, electronics, control and communications in a compact device that can be easily assembled, reducing significantly the design and development effort; 2) these actuators can be controlled in position/speed, allowing the generation of a wide variety of flapping patterns with desired amplitude, frequency, offset angle; and 3) the diversity of servo models commercially available facilitates the development of a customised aerial platform. However, since these actuators are intended to provide high torque rather than high speed (reduction ratios around 200:1 are usual), the flapping frequency will be limited by the maximum servo speed ($\omega_a^{max} \sim 6$ rad/s).

B. Winged Aerial Robot with 2 SFEs

A prototype of winged aerial robot built with two SFE modules is developed and illustrated in Figure 1. The frame structure consists of a 80 cm length, 6 mm section carbon fibre tube that is attached to the SFE modules through the Ruland aluminium collars. These are separated 30 cm, placing the control electronics in the space between them. A 2S 800 mAh LiPo battery is located on the front part of the first SFE so the center of mass is close to the border of the wing, which is necessary for pitch control. The wing structure consists of two 75 cm length, 4 mm section carbon fibre rods attached to the servo horns, and a light nylon cloth that is stretched introducing four thin rods (1 mm section) between the servo rods. A certain aerodynamic profile in the wing is achieved pretensioning these thin rods using strings tied at the ends. The tail is actuated in pitch by a Graupner DES 428 BB MG digital servo (9.5 g weight). A vertical stabiliser is required in the tail to avoid the lateral instability.

C. Components and Architecture

The winged aerial robot implements the hardware architecture depicted in Figure 3. This consists of two groups of smart servo actuators, one per SFE module, with different ID's, connected in daisy chain through an USART interface to the STM32F303 board where the main control program is executed. The tail servo is a Graupner DES 428 BB MG controlled by a PWM signal directly managed by the microcontroller. The orientation of the body frame is measured with a BNO055 IMU through an I^2C communication, introducing an XBee module using a 802.15.4 protocol at 2.4 GHz for the wireless communication with the ground control station, and a FLYSKY radio Rx for controlling manually the platform. The system is fed with a LiPo 2S battery. The control program of the microcontroller is developed in C/C++ using the Atollic True Studio IDE and the STM32 Cube tool.

IV. Aerodynamic Modelling and Control

A. Kinematics

The kinematic model of the winged aerial robot is depicted in Figure 4, representing the reference frames along with the position vectors and the geometric parameters of interest, illustrated on a 3-SFE modules prototype. Two coordinate systems are considered: the Earth fixed frame $\{E\}$ (inertial), and the body fixed frame $\{B\}$ attached to the center of mass (CoM) of the platform, whose position and rotation are denoted as ${}^E\vec{r}_B \in R^3$ and ${}^E\vec{R}_B(\phi, \theta, \psi)$, respectively. The SFE modules are represented by subscript $j = \{1, 2, ...N\}$, whereas superscript $i = \{1, 2\}$ will denote the left-right wing. In this way, q_j^i is the rotation angle of the i-th wing in the j-th SFE, and q_{tail} is the pitch angle of the tail. The deflection angle of each wing section is defined as the difference between the rotation angle of two consecutive servos, that is, $q_j^i - q_{j-1}^i$.

B. Aerodynamics

The winged aerial robot presented in this paper extends the control of the flapping motion compared to [3], [2] thanks to the use of smart servo actuators, allowing the generation of patterns with desired dihedral angle, flapping amplitude and frequency, or wing orientation, as illustrated in Figure 2. These control variables can be exploited to improve the aerodynamic performance of the robot. In order to do that, this section provides some basic ideas of the aerodynamic behaviour of the wings for different configurations.

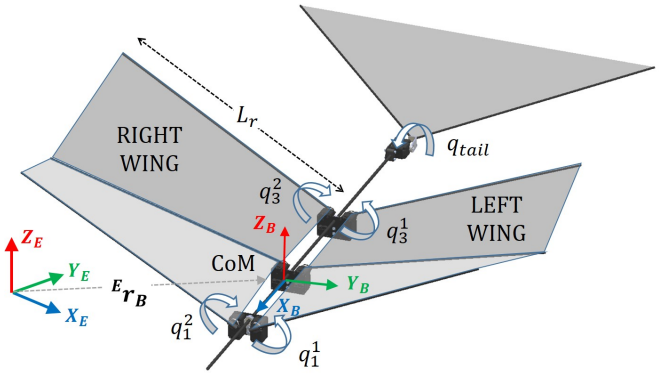

Figure 4. Kinematic model of a winged aerial robot with three SFE.

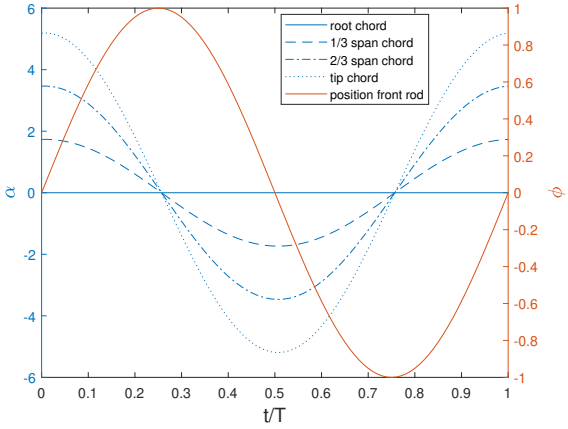

Figure 5. Pitching variation (α) generated at the wing with 30 of amplitude and 5 of phase difference (ϕ) within front and back rod at different chords along the wingspan. In the right axis, position of the front rod with respect to its maximum amplitude.

The generation of appropriate flapping motions is one of the main challenges in this kind of platforms. There are several of aerodynamic studies about flapping wings, both theoretical [13], [14] and experimental [15]. They conclude that optimal efficiency is obtained at Strouhal number around 0.3. Note that this number corresponds to frequencies around 4 Hz at an amplitude of 30 and an airspeed of 10 m/s. However, if the drag of the vehicle is not minimised, the ornithopter requires more thrust to fly. In this case, higher amplitudes or frequencies are needed. Reducing the airspeed is not advisable, as bigger angles of attack would be needed to maintain the flight, resulting in a drag increase.

An advantage of the design proposed here is the possibility of generating different flapping patterns to optimise the aerodynamic performance. By adding a deflection angle between the leading edge and the trailing edge actuators, a pitching movement is generated, which leads to a better aerodynamic performance. Note that the pitching movement generated with this phase difference does not have the same maximum angle for all the span, but it grows from 0 to a maximum in the wingtip, as it can seen in Figure 2, and also analytically in Figure 5. Also, the flapping movement is delayed 90 with the pitching movement, which corresponds to an optimum according to previous aerodynamic studies [15].

Another advantage of the design is the control possibilities of the prototype, which can use the wings to generate both pitching and rolling moment. Moving down symmetrically both back rods, makes the effective angle of attack of the wing to grow, causing a pitching moment which leads to a different trim angle. In addition, moving one rod back up and the other down asymmetrically, leaves the effective angle of attack equal, but it generates a difference of lift force between both wings and, consequently, a roll moment which allows the device to make turns. Correct adjustment of those control variables may allow the need of the tail actuator, leaving it just as stabilising surface.

In the case of gliding, the control capabilities of the wing can be estimated, considering the lifting line theory, resulting in a lift control power of

$$C_{L_{\delta_f}} = \frac{\Delta L}{\frac{1}{2}\rho S V^2 \Delta\delta_f} = 2.98; \tag{5}$$

being ρ the air density, S the wing surface and V the airspeed. $\Delta L/\Delta\delta_f$ represents the increase in lift force generated by an unitary symmetric deflection of the back rod downwards. Similarly, lateral control power can also be estimated,

$$C_{l_{\delta_a}} = \frac{\Delta l}{\frac{1}{2}\rho S V^2 b \Delta\delta_a} = 1.59; \tag{6}$$

where b is the wingspan and, in this case, $\Delta l/\Delta\delta_a$ computes the roll moment generated in the vehicle by an unitary anti-symmetric deflection of the back rod.

C. Flapping-Wing Frequency Characterisation

It is also interesting, from the aerodynamic theories, to estimate the moment which the actuators have to overcome. For a first order approximation, moment can be considered to be produced mainly due to lift contributions. In this case, we have used Theodorsen formulation of the lift of an oscillating airfoil [13], adapted for finite wings [16]:

$$C_L = 2\pi k h_0 \left(G(k)\cos(2\pi f t) + F(k)\sin(2\pi f t)\right)\frac{\mathcal{AR}}{\mathcal{AR}+2} + \pi k^2 h_0 \cos(2\pi f t) \tag{7}$$

where the reduced frequency $k = 2\pi f c/2U$ is computed from the flapping frequency f, the wing chord c, and the airspeed U, whereas $\mathcal{AR}$ is the aspect ratio, and h_0 is the flapping amplitude. The results shown in Figure 6 evidence that the moment increases more with the frequency than with the amplitude. Therefore, and according to the parametrization defined in Section II-A, it is preferable to consider servo actuators with higher angular speed rather than high torque.

D. Control Modes: Gliding and Flapping

Two flight modes are implemented in the winged aerial robot: gliding and flapping. The gliding mode is defined by the dihedral angle of the wings, which can be adjusted in the range from 0 to 90 degrees with respect to the horizontal axis (Y_B). The tail servo will be used to control the platform in pitch

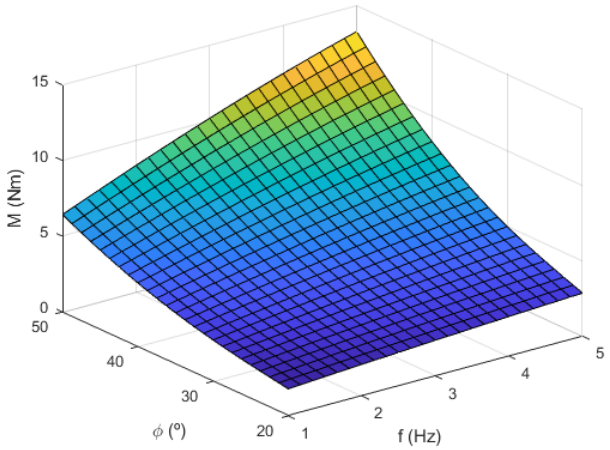

Figure 6. Maximum torque of the servo as function of the frequency and the amplitude for an airspeed of $5\,\mathrm{m/s}$

Figure 7. Sequence of images showing the gliding of the winged aerial robot along with the travelled distance.

angle θ, whereas the roll angle ϕ will be controlled through the deflection of the wings, that is, varying the relative rotation angle of two consecutive SFEs.

The flapping mode is implemented generating a sinusoidal rotation pattern in each of the servos in the following way:

$$q_j^i(t) = A_0 + A \cdot sin(2\pi f \cdot t + \theta_p) + C \tag{8}$$

where A_0 is the dihedral angle, A is the flapping amplitude (0 - 90 deg), f is the flapping frequency (0 - 5 Hz), and θ_p is the phase of the wing rods. The difference in the phase of two consecutive SFE modules modifies the deflection angle of the wings during the upstroke and downstroke transition, and with it, the generated lift and drag forces, although this analysis is out of the scope of the paper. The term C_ϕ is the correction term for roll compensation:

$$C_\phi = (-1)^j k_\phi \cdot (\phi_{ref} - \phi) \;\; ; \;\; \phi_{ref} = 0 \tag{9}$$

Pitch control is achieved by implementing a proportional law where the tail angle (q_{tail}) is calculated as described in Equation (10), where k_θ is the proportional gain, and θ_{ref} is the reference pitch angle whose value, around $10°$, is determined empirically to maintain the lift during the gliding.

$$q_{tail} = k_\theta \cdot (\theta_{ref} - \theta) \tag{10}$$

V. Experimental Results

A. Gliding Tests

Outdoor flight tests have been conducted to evaluate the ability of the winged aerial robot to glide straight, controlling the orientation in pitch with the tail servo and the roll angle through the deflection of the wings, implementing the proportional controller given by Eq. (9). The attitude reference in pitch is determined experimentally and set to 10 degrees to produce lift with relatively low drag. The deviations in roll are controlled rotating the rear rods with respect to the front rods in the wings to produce a moment in this angle. Figure 7 shows

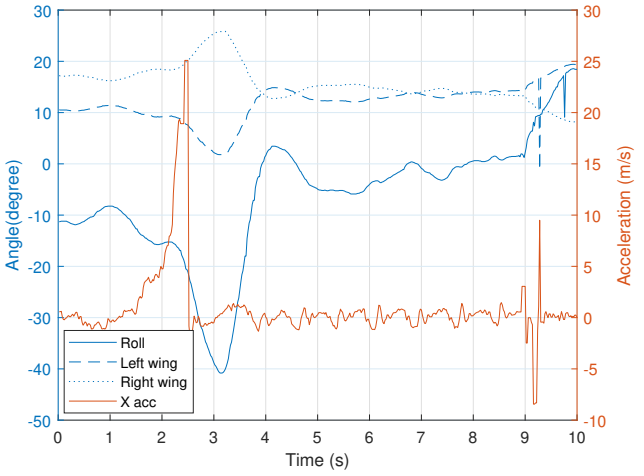

Figure 8. Gliding test with roll control using the deflection of the wings.

a sequence of images from the video attachment that validates the proposed design and the gliding capability, whereas Figure 8 represents the evolution of the signals of interest, including the position reference of the rear rods of the left/right wings. The acceleration, referred to the body frame $\{B\}$, is useful in the identification of the launching and landing events, which allows the calculation of the flight time (6.5 sec). The aerial robot is launched with 20 m/s^2 acceleration, travelling 25 m with a mean speed around 3.8 m/s. As it can be seen in Figure 8, the deflection of the wings around t = 3 s allows to correct the initial 40 deg deviation in roll, which validates the proposed controller. Previous experiments revealed the need to incorporate the vertical stabiliser in the tail to avoid the drift and instability in the roll/yaw angles associated to the lateral dynamics.

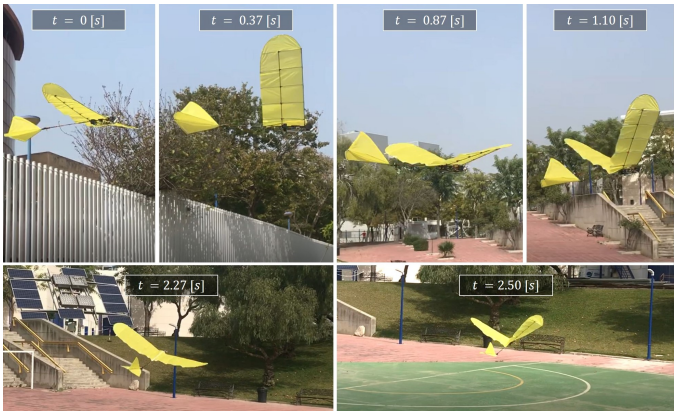

Figure 9. Sequence of images showing the flapping of the winged robot.

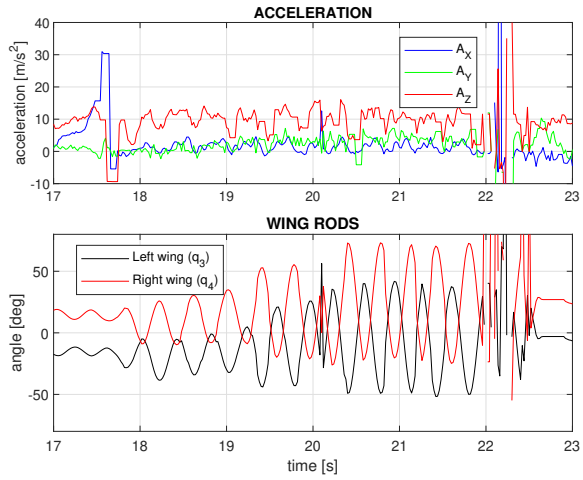

Figure 10. Flapping wing flight test. Acceleration (up) and left/right wings angle reference (down). The robot is launched at t = 17.5 s and lands at t = 22 s.

B. Flapping Test

The prototype is also evaluated in an outdoor flight test flapping the wings, as it can be seen in the video attachment. The sinusoidal flapping pattern given by Eq. (8) is generated for both wings, with $A = 30$ deg amplitude, $A_0 = 10$ deg dihedral angle, and $f = 3$ Hz frequency. Figure 9 shows a sequence of images taken from the video experiment, whereas Figure 10 represents the acceleration of the robot along with the servo references of the left and right wing rods. The X-axis acceleration peak at $t = 17.5$ s corresponds to the launch, and the peak at $t = 22$ s is the landing. The prototype flies a distance around 23 m in a 4.5 seconds interval, resulting in a mean speed around 5 m/s (higher than the gliding speed), implementing the same controllers for roll and pitch.

VI. Conclusion and Future Work

This paper presented a modular approach for the development of flapping-wing aerial robots employing smart servo actuators. This allows to simplify the manufacturing and enhance the control capabilities through the orientation of the wings, generating flapping motions with desired amplitude, dihedral angle, frequency and phase. Gliding and flapping tests have been conducted in outdoors with a prototype built with two SFE, controlling the roll angle with the wings and the pitch angle with the tail. The prototype is characterised by its low power consumption (20 W) and relatively low speed (5 m/s), which facilitates the perching and landing to conduct inspection or manipulation operations.

As future work, the control of the prototype will be improved to achieve a more stable and accurate flight with desired trajectories, evaluating and comparing the performance of a 3-SFE platform.

VII. Acknowledgements

This work has been funded by the ERC Advanced Grant GRIFFIN, Action 788247, and the AERIAL-CORE (H2020-2019-871479) project from the European Commission.

Authors wish to thank Marta Quevedo for her support in the realisation of the experiments.

References

[1] T. N. Pornsin-Sirirak, Y.-C. Tai, C.-M. Ho, and M. Keennon, "Microbat: A palm-sized electrically powered ornithopter," in *Proceedings of NASA/JPL Workshop on Biomorphic Robotics*, vol. 14. Citeseer, 2001, p. 17.

[2] J. Gerdes, A. Holness, A. Perez-Rosado, L. Roberts, A. Greisinger, E. Barnett, J. Kempny, D. Lingam, C.-H. Yeh, H. A. Bruck *et al.*, "Robo raven: a flapping-wing air vehicle with highly compliant and independently controlled wings," *Soft Robotics*, vol. 1, no. 4, pp. 275–288, 2014.

[3] G. A. Folkertsma, W. Straatman, N. Nijenhuis, C. H. Venner, and S. Stramigioli, "Robird: a robotic bird of prey," *IEEE robotics & automation magazine*, vol. 24, no. 3, pp. 22–29, 2017.

[4] A. Roshanbin, H. Altartouri, M. Karásek, and A. Preumont, "Colibri: A hovering flapping twin-wing robot," *International Journal of Micro Air Vehicles*, vol. 9, no. 4, pp. 270–282, 2017.

[5] Y. Chen, H. Wang, E. F. Helbling, N. T. Jafferis, R. Zufferey, A. Ong, K. Ma, N. Gravish, P. Chirarattananon, M. Kovac *et al.*, "A biologically inspired, flapping-wing, hybrid aerial-aquatic microrobot," *Science Robotics*, vol. 2, no. 11, 2017.

[6] B. Theys, G. Dimitriadis, P. Hendrick, and J. De Schutter, "Influence of propeller configuration on propulsion system efficiency of multi-rotor unmanned aerial vehicles," in *2016 international conference on unmanned aircraft systems (ICUAS)*. IEEE, 2016, pp. 195–201.

[7] P. E. Pounds and W. Deer, "The safety rotor—an electromechanical rotor safety system for drones," *IEEE Robotics and Automation Letters*, vol. 3, no. 3, pp. 2561–2568, 2018.

[8] "Erc advanced grant griffin project," https://griffin-erc-advanced-grant.eu/, accessed: 2020-08-18.

[9] A. Suarez, M. Perez, G. Heredia, and A. Ollero, "Small-scale compliant dual arm with tail for winged aerial robots," in *2019 IEEE/RSJ International Conference on Intelligent Robots and Systems (IROS)*. IEEE, 2019, pp. 208–214.

[10] A. Suarez, P. Grau, G. Heredia, and A. Ollero, "Winged aerial manipulation robot with dual arm and tail," *Applied Sciences*, vol. 10, no. 14, p. 4783, 2020.

[11] A. Ramezani, X. Shi, S.-J. Chung, and S. Hutchinson, "Bat bot (b2), a biologically inspired flying machine," in *2016 IEEE International Conference on Robotics and Automation (ICRA)*. IEEE, 2016, pp. 3219–3226.

[12] J. J. Videler, *Avian flight*. Oxford University Press, 2006.

[13] T. Theodorsen, "General theory of aerodynamic instability and the mechanism of flutter," *Technical Report TR 496, NACA*, 1935.

[14] I. E. Garrick, "Propulsion of a flapping and oscillating airfoil," *Technical Report TR 567, NACA*, 1936.

[15] M. F. Platzer, K. D. Jones, J. Young, and J. C. S. Lai, "Flapping wing aerodynamics: Progress and challenges," *AIAA Journal*, vol. 46, no. 9, pp. 2136–2149, 2008.

[16] A. J. Smits, "Undulatory and oscillatory swimming," *Journal of Fluid Mechanics*, vol. 874, pp. 1–44, 2019.